Proceedings of the Korean Nuclear Society Autumn Meeting
Kori, Korea, May 2000

Evaluation of nucleon scattering cross section of ^{58}Ni using the coupled-channels analysis with the soft-rotator model

Young-Ouk Lee, Choong-Sup Gil, Jeong-Yeon Lee and Jonghwa Chang
Korea Atomic Energy Research Institute
P.O. Box 105 Yusong, Taejon 305-600, Korea

Efrem Sh. Sukhovitski
Radiation Physics and Chemistry Problems Institute
220109, Minsk-Sosny, Belarus

abstract

Coupled channel anaysis was applied based on the soft-rotator model to evaluate neutron and proton scattering cross sections of ^{58}Ni. It was found that the model could describe the collective level structure of ^{58}Ni, which does not exhibit the typical rotational nor harmonic vibrational structure, up to excitation energy of 4.5 MeV modestly. The nucleon scattering cross sections were described up to 150 MeV reasonably well by the coupled-channles method with a coupling scheme constructed consistent to the nuclear structure of ^{58}Ni.

I. Introduction

The ^{58}Ni nucleus has attracted a good deal of attentions from applicational points of view since it is a component of the structure materials of nuclear reactors and D-T fusion device. Furthermore, for design of the accelerator-driven nuclear wastes transmutation facilities, not only neutron but also proton induced cross sections of ^{58}Ni are requested for incident energies up to 150 MeV.

On the fundamental side, the ^{58}Ni nucleus is considered normally as a vibrational nuclei, and nucleon interaction cross section calculations, using coupled-channels or DBWA formalism, are performed involving the harmonic vibrational model. However the ^{58}Ni nucleus does not exhibit a level spectrum characteristics to the harmonic vibration; the degeneracy of the two-phonon triplet is broken considerably, showing that the anharmonicity effect is large in this nucleus. Furthermore the energy splitting of the yrast 0^+, 2^+, 4^+ and 6^+ levels is very irregular to be considered as harmonic vibrational states. Therefore, the calculation of nucleon interaction cross sections cannot ignore the effect of such anharmonicity, which implies that the nuclear structure information is very important for a correct understanding of the interaction cross sections of this nucleus.

In the present work, we employ the soft-rotator model to desribe the collective level structure of ^{58}Ni nucleus. This model was found to be very successful in describing the nuclear structure, nucleon interaction and B(E2) transitions for both very light (^{12}C)[1, 2] and heavy (actinide) [3] nuclei. It is therefore a matter of big interest to see whether or not the soft-rotator model[4, 5], frequently employed for rotational nuclides successfully, is applicable in the mass region of ^{58}Ni where the collective structure is more vibrational in nature. To realize our purpose we used a very small equilibrium deformation, but a very large softness to the quadrupole deformation, so that the ground-state band could describe the corresponding band in the U(5) symmetry limit of the IBM-1[6]. Until now, no consistent attempts have been given to describe the low-lying collective level structure and nucleon scattering data of ^{58}Ni in such a unified framework. The purpose of this work is to carry out such an analysis intending to use the results for high energy nuclear data evaluation for ^{58}Ni .

II. Coupled channels formalism based on the soft-rotator model

The soft-rotator model was developed as an extension of the Davydov-Chaban model[7] which takes account of the β-vibration in non-axial soft rotational nuclei. Here, the word "soft" denotes a possibility of stretching during the rotation. The present version of the soft-rotator model includes the non-axial quadrupole, octupole and hexadecapole deformations, and the β_2-, β_3- and γ- vibrations[3–5]. This model has been extensively applied for similar analyses in heavier and lighter mass regions. The soft-rotator model and its application as a base for creating reliable and self-consistent coupling scheme, built on the wave functions of soft-rotator nuclear model Hamiltonian, for coupled-channels (CC) optical model calculations are described elsewhere[8]. In this model, the deformed nuclear optical potential arises from deformed instant nuclear shapes, taken to a standard form:

$$R(\theta',\varphi') = R_i \left\{ 1 + \sum_{\lambda\mu} \beta_{\lambda\mu} Y_{\lambda\mu}(\theta',\varphi') \right\} \tag{1}$$

with $\lambda \geq 2$, presented with evident dependences on the nuclear collective variables $\beta_{\lambda\mu}$ (deformations). Usually multipoles of deformed nuclear potential are determined, expanding it in Taylor series, considering $(\sum_{\lambda\mu} \beta_{\lambda\mu} Y_{\lambda\mu}(\theta',\varphi'))$ small:

$$V(R) \;=\; V(R_i) \;+\; \sum_{t=1}^{max} \left.\frac{\partial^t V}{\partial R^t}\right|_{R=R_i} \frac{R_i^t}{t!} (\sum_{\lambda\mu} \beta_{\lambda\mu} Y_{\lambda\mu}(\theta',\varphi'))^t. \tag{2}$$

Enhancement of the coupling strength compared with the rigid-rotator model arises because the dynamic variables in deformed nuclear optical potential expansion are averaged over the wave functions of the appropriate collective nuclear shape motions, given by the soft-rotator model Hamiltonian solutions, describing rotational-vibrational states of non-axial deformed deformable nuclei. Such enhancement is equal to $\langle i|\beta_\lambda^t|f\rangle/\beta_{\lambda G.S.}^t$ and this ratio is usually greater than unity as a soft-rotating nucleus is stretched due to the centrifugal force, so that equilibrium deformations $\beta_{\lambda I\tau}$ for states with higher spins I are greater than equilibrium ground state (G.S.) deformation $\beta_{\lambda G.S.}$ (here $\beta_\lambda^2 = \sum_\mu \beta_{\lambda\mu}\beta_{\lambda\mu}^*$ is the measure of nucleus deformation with multipolarity λ). Such enhancements are different for different combinations of initial $|i\rangle$ and final $|f\rangle$ states, and also depend on the powers of potential expansion t. In this way, the soft-rotator model predicts the redistribution of coupling strength, i.e., the particle current between the channels, which in turn changes the estimates of direct level excitation cross sections compared with the rigid rotor of harmonic vibrational model.

The optical potential is taken to be a standard form:

$$\begin{aligned} V(r) \;&=\; -V_R f_R(r) + i\left\{ 4W_D a_D \frac{d}{dr} f_D(r) - W_V \; f_V(r) \right\} \\ &\quad + \left(\frac{\hbar}{\mu_\pi c}\right)^2 (V_{SO} + iW_{SO}) \frac{1}{r}\frac{d}{dr} f_{SO}(r) \boldsymbol{\sigma}\cdot\mathbf{L} + V_{Coul}(r), \end{aligned} \tag{3}$$

with the form factors given as

$$f_i \;=\; \left[1 + \exp\left(r - R_i\right)/a_i\right]^{-1}, \qquad R_i \;=\; r_i A^{1/3}, \qquad i = R, V, D \;\text{ and }\; so. \tag{4}$$

The subscripts $i = R, V, D$ and so in eqs. (3) and (4) denote the real volume, imaginary volume, imaginary surface and real spin-orbit potentials, respectively. The strength of these potentials are assumed to have the following form,

$$V_R \;=\; V_R^0 + V_R^1 E_p + V_R^2 E_p^2 + (-1)^{Z'+1} C_{viso}(A-2Z)/A + C_{coul} Z Z'/A^{1/3},$$

$$\begin{aligned} W_D &= W_D^0 + W_D^1 E_p + (-1)^{Z'+1} C_{wiso}(A-2Z)/A, \\ W_V &= W_V^0 + W_V^1 E_p, \\ W_{SO} &= W_{SO}^0 + W_{SO}^1 E_p \end{aligned} \tag{5}$$

where Z', Z are charges of incident particle and target nucleus, and A the target mass number. The symbol E_p denotes the energy of the projectile and potential slopes W_D^1 and W_V^1 may change at $E_p = E_{change}$. Noticeable energy losses due to collective levels excitation of the ^{58}Ni nuclei as compared with the nucleon incident energies involved in the analysis request the dependence of local optical potential for different channels, which was taken into account for diagonal potential elements as:

$$V_{if} = V\left(E_p - E_i\right)$$

and for non-diagonal as:

$$V_{if} = V\left(E_p - \frac{E_i + E_f}{2}\right),$$

where i and f denote initial and final channels, while E_i and E_f the corresponding level energies. As we intend to analyze neutron and proton scattering data simultaneously, our potential contains a term $C_{coul}ZZ'/A^{1/3}$ describing the Coulomb correction to the real optical potential and isospin terms $(-1)^{Z'+1}C_{viso}(A-2Z)/A$ added to real and $(-1)^{Z'+1}C_{wiso}(A-2Z)/A$ added to imaginary surface potentials.

III. Estimation of soft-rotator nuclear model Hamiltonian parameters, describing low-lying ^{58}Ni collective levels

SHEMMAN code[1, 10] was used to adjust the soft-rotator nuclear model Hamiltonian parameters, allowing the description of the experimentally observed low-lying collective levels of ^{58}Ni nucleus. Initial assignment of the soft-rotator model quantum numbers to the experimentally observed low-lying collective levels of ^{58}Ni was done in our standard approach. We considered yrast levels with spins and parities $J^\pi = 0_1^+$ (G.S.), 2_1^+(1.454 MeV) and 4_1^+(2.459 MeV) to be members of the ground state rotational band with $K \simeq 0$, n_{β_2}=n_{β_3}=n_γ=0. Second J^π =2_2^+(2.775 MeV) and first J^π =3_1^+(3.420 MeV) levels were assigned as members of the $K \simeq 2$, n_{β_2}=n_{β_3}=n_γ=0 band. This allowed us to find initial soft-rotator Hamiltonian parameters describing the chosen experimental levels. The initially adjusted Hamiltonian parameters made possible the assignment of the soft-rotator model quantum numbers to other observed levels, considered as levels of G.S. $K \simeq 0$, n_{β_2}=n_{β_3}=n_γ=0; $K \simeq 2$, n_{β_2}=n_{β_3}=n_γ=0 and $K \simeq 0$, n_{β_2}=1, n_{β_3}=n_γ=0 bands.

After ^{58}Ni experimental levels were assigned in this way, the final nuclear Hamiltonian parameters were adjusted using SHEMMAN code[1, 10]. The rotational nor vibrational structure is not very prominent in the case of ^{58}Ni nuclide, nevertheless we could describe the first five low-lying collective levels and some others lying above, necessary for creating a coupling scheme of CC calculations, with an accuracy of about 10%. For most of these levels the accuracy is better, except the levels considered as first levels of $K \simeq 0$, n_{β_2}=1, n_{β_3}=n_γ=0 band with $J^\pi = 0_2^+$(2.942 MeV) and 2_5^+(3.898 MeV). For instance the first excited 2_1^+ level with measured energy of 1.454 MeV is predicted by the model at 1.269 MeV, the 4_1^+ level (E$_x$=2.459 MeV) is predicted at 2.615 MeV, the 2_2^+ level (E$_x$=2.775 MeV) at 2.806 MeV and the 3_1^+ level (E$_x$=3.420 MeV) at 3.412 MeV. The model predicts that the experimentally measured level with 3.934 MeV excitation energy, the spin of which is not assigned, to be the J^π =6_1^+ level of the G.S. band, with a predicted energy of 3.968 MeV. The second J^π =0_2^+ level with energy 2.942 MeV was described as the head of $K \simeq 0$, n_{β_2}=1, n_{β_3}=n_γ=0 band. However, the predicted energy 2.134 MeV is

not in good agreement with experimental value of 2.942 MeV. The level with $J^\pi = 2^+$ of this band predicted with energy 3.615 MeV is assigned to the experimental $J^\pi = 2_5^+$ (3.898 MeV) one. The level with spin and parity $J^\pi = 1_1^+$ (2.901 MeV) is not of a collective nature and we were not trying to describe it. The level with $J^\pi = 4^+$ found at 4.299 MeV is described as the member of $K \simeq 2$, n_{β_2}=n_{β_3}=n_γ=0 for which the model predicts a 4.157 MeV excitation energy. The negative parity level $J^\pi = 3_1^-$(4.474 MeV) with predicted energy 4.452 MeV is described as the member of negative parity $K \simeq 0$, n_{β_2}=n_{β_3}=n_γ=0 band, the energy of which is described by energy splitting for symmetric and antisymmetric β_3 oscillator function solutions, determining positive and negative parity collective states of the soft-rotator model accordingly[3].

Figure 1 demonstrates the comparison of experimental and predicted ^{58}Ni level schemes. The nuclear Hamiltonian parameters allowing demonstrated level prediction are given in Table 1. One can see that ^{58}Ni demonstrates large softness $\mu_{\beta_{20}} = 1.9095$. It is consistent with the well known fact that nuclei with N and Z in the vicinity of magic numbers can be considered spherical for G.S. and are deformed in excited states, for our model that means that such ^{58}Ni nuclei is very soft to β_2 deformations.

IV. Estimation of the optical potential parameters

Nuclear wave functions of the soft-rotator model with the adjusted nuclear Hamiltonian parameters, given in Table 1, were used to construct the coupling among seven collective ^{58}Ni levels (0^+(G.S.), 2_1^+(1.454 MeV), 4_1^+(2.459 MeV), 2_2^+(2.775 MeV), 0_2^+(2.942 MeV), 2_5^+(3.898 MeV) and 3_1^-(4.475 MeV)) in the coupled-channels (CC) calculations using OPTMAN code[1, 10, 11]. Preliminary numerical results showed that the inclusion of additional levels influences the numerical results by much less than experimental errors. Levels coupled in current calculations and the coupling scheme are presented in Fig. 2. Each pair of levels having the same parity and levels themselves are coupled by all possible even multipoles with angular momentum transfer up to $8\hbar$ and by odd multipoles with angular momentum transfer up to $7\hbar$ for pairs of levels with different parity. The Coulomb interaction enhances the coupling in all the pairs of levels except between 0^+(G.S.) and 0_2^+(2.942 MeV) states (as square terms which lead to Coulomb potential zero multipoles were truncated), so these levels were coupled only by nuclear potential. We must emphasize that levels from various bands are coupled in our model not only with the ground state band, but also with each other without any additional assumptions. Such a feature is absent in most of the previous analyses.

Experimental data used for the optical potential search were taken from the EXFOR database [12]. The following experimental neutron scattering data was involved in the current analysis: angular distribution measurements of neutrons scattered on G.S. and the first 2^+ excited level for eleven incident energies from 4.5 to 10 MeV of Smith et al.[13]; analogous experimental results for incident neutron energies 7.904, 9.958, 11.952 and 13.941 MeV of Guss et al.[14]; elastic scattering angular distribution measured for 14.7 MeV incident energy by Tutubalin et al.[15]; scattered neutron angular distribution measurements for G.S. and the first 2^+ excited level for 16.934 MeV incident energy of Perdoni et al.[16] and experimental scattered neutrons angular distribution data for G.S., the first $2^+$and 3^- levels at 24 MeV incident energy of Yamanouti et al.[17].

Proton interaction data is rather scarce, so we can use the 30.3 MeV incident proton elastic scattering angular distributions measurement of Ridley et al.[18]; data on inelastic proton scattering angular distributions by the first 2^+ and 3^- levels at 39.7 MeV by Stovall et al.[19]; 40 MeV incident proton elastic scattering angular distributions measured by Blumberg et al.[20], supplemented by measurements of angular distributions for the first 2^+ and 3^- levels for the same incident energy by Fricke et al.[21] and Fulmer et al.'s elastic scattering angular distribution measured for 61.4 MeV incident energy[22]. We can use for comparison the scattering

data[23–25] for 20, 20.4, 24.6 and 65 MeV incident energies, which have no reliable experimental errors in EXFOR because they were compilied by reading the graphs presented in publications.

Detailed information about the data used in the CC analysis can be found in Table 2. Evaluated neutron strength functions $S_{l=0,1}$ and ^{58}Ni total neutron interaction cross section σ_{tot}, based on References [13, 26] up to 20 MeV incident neutron energies and natural Ni total cross section corrected for other Ni isotopes contamination (accounting that σ_{tot} is proportional to $A^{2/3}$ for different isotopes) were also used. The data from Ref.[27–30] covering the entire region of incident neutron energies necessary, were also used in optical potential adjustment. One can see that we did not include scattered angular distribution data for nucleon interaction energies below 7 MeV in the adjustment. As checked, for such incident energies we could not guarantee that compound interaction contribution to angular distributions is less than the experimental errors and can be neglected. For lower energies, energy loss even for the first 2_1^+(1.454 MeV) excited level decreases the nucleon energy in outgoing scattering channels to the energy region with resonance structure (experimentally observed in total cross section for neutrons, see Fig.3) which can influence the results of the potential search. We therefore could assumed that the interaction of nucleons with ^{58}Ni for experimental data involved for optical potential search proceeds only *via* the direct mechanism, which can be described by the optical model.

Using one of the OPTMAN code[1, 10, 11] options, the optical potential parameters were searched by minimizing the quantity χ^2 defined by

$$\chi^2 = \frac{1}{N+M+2}\left[\sum_{i=1}^{N}\frac{1}{K_i}\sum_{j=1}^{K_i}\left(\frac{d\sigma_{ij}/d\Omega_{calc}-d\sigma_{ij}/d\Omega_{exp}}{\Delta\sigma_{ij}/d\Omega_{exp}}\right)^2+\sum_{i=1}^{M}\left(\frac{\sigma tot_{cal_i}-\sigma tot_{eval_i}}{\Delta\sigma tot_{eval_i}}\right)^2+\sum_{i=0}^{1}\left(\frac{S_{l_{cal_i}}-S_{l_{eval_i}}}{\Delta S_{l_{eval_i}}}\right)^2\right],$$

where N is the number of experimental scattering data sets, K_i the number of angular points in each data set, M the number of energies, for which the experimental neutron total cross section is involved. During the optical parameter search, the parameters of the nuclear Hamiltonian were fixed except for μ_{γ_0}; it was impossible to determine this Hamiltonian parameter by analyzing the level scheme alone, since no levels with $n_\gamma \geq 1$ are observed in our analysis of ^{58}Ni level scheme due to our assignment.

V. Results and discussion

The adjusted optical potential parameters, allowing the best fit to the the experimental data, are presented in Table 3. It is evident that the total neutron cross section data for ^{58}Ni[13, 26–30] in the energy region from 3 to 150 MeV (Fig. 3) and available experimental neutron and proton scattering data (Figs. 4-9) are described fairly well by the present model in a consistent manner. The overall χ^2 is 4.5, that means experimental data is described on average within approximately two experimental errors. We consider such a quality of description acceptable, yet some comments are necessary.

One can see (Fig. 6), that our calculations underestimate angular distributions of neutrons with incident energy 5.9 MeV, scattered on the 2^+(1.454 MeV) level. For the same reason predicted elastic scattering for this incident energy underestimates experimental values, predicting a deeper valley for about 135 degree scattering angles (Fig.4). It proves, as discussed above, that the contribution of the compound scattering mechanism for such energies couldn't be neglected. This was the reason not to include experimental scattering data for incident energies below 7.5 MeV in the optical potential parameter search.

Experimental angular distributions of protons scattered by 2^+(1.454 MeV) and especially 3^-(4.474 MeV) levels[19, 21], which are measured for almost the same incident energies 39.7 and 40 MeV accordingly, are in contradiction (see Figs. 7,9). We relied on Stovall et. al's data[19] in the potential parameters search due to the reason mentioned above. This determines lower predicted angular distribution values for 3^- level excitation as compared with[21] for 40 MeV and [24] for 24.6 MeV incident energies.

Above we mentioned redistribution of coupling strength in different channels without any additional assumptions as the inherent feature of the (CC) approach builds on wave functions of soft-rotator Hamiltonian. The "equilibrium"quadrupole ^{58}Ni deformation β_{20} was found to be 0.0788 in this analysis , which gives an "effective" deformation 0.195, when averaged by β_2 oscillation functions, resulting in a 0.925 fm "effective" deformation length for direct excitation of the 2^+(1454 MeV) level. The latter value can be compared with 0.9 fm used in the harmonic oscillator model analysis of ^{58}Ni angular distributions[31]. This fact shows the softness of ^{58}Ni to such a degree-of-freedom, feature ignored in the frequently employed rigid-rotator model. The result of our $\langle 0^+|\beta_2^2|0_2^+\rangle$ value determining one step excitation of the 0_2^+ (2.942MeV) level is 15 % lower than $\langle 0^+|\beta_2^2|2_1^+\rangle$, while $\langle 0^+|\beta_2|2_1^+\rangle\langle 2_1^+|\beta_2|0_2^+\rangle$ determining two step excitation strength is 35% lower. This results in the lower coupling strength decreasing the predicted 0_2^+ level excitation value compared with the model assuming a constant β_2 value, which requests for such models appropriate determination of β_2 for each pair of channels. This is what we call the redistribution of coupling strength, which leads to the redistribution of nucleon current in a different channel without additional assumptions. It is the result of stretching a soft rotating ^{58}Ni nucleus due to rotations incorporated in the present model.

VI. Concluding remarks

The soft-rotator nuclear model and CC method with a coupling based on the soft-rotator model wave functions were applied to analyze available ^{58}Ni experimental total, nucleon scattering and collective level structure in a consistent fashion. It was found that the model gives a modest success in describing the collective low-lying level structure of ^{58}Ni which exhibits neither the typical rotational nor the vibrational spectra, while the nucleon interaction data were described reasonably well up to 150 MeV. It is recommended that the results of the present work be used for evaluation of scattering cross sections of structural material for the nuclear fission/fusion reactors as well as the accelerator-driven nuclear wastes transmutation facilities,

Acknowledgements

This work was performed under the auspices of Korea Ministry of Science and Technology as one of the long-term nuclear R&D programs. One of the authors (E.Sh.S.) is grateful to the Korea Institute of Science and Technology Evaluation Planning for providing financial support, Korea Atomic Energy Research Institute for offering the opportunity to stay at KAERI and for the hospitality of KAERI Nuclear Data Evaluation Laboratory team, which made this work possible for him.

Table 1: The nuclear Hamiltonian parameters adjusted to reproduce the experimental level schemes

$\hbar\omega_0 = 1.2470$		
$\mu_{\beta_{20}} = 1.9095$	$\mu_{\gamma_0} = 0.4000$	$\gamma_0 = 0.6272$
$a_{32} = 0.0001$	$\gamma_4 = 0.14410$	$\delta_4 = 0.6971$
$a_{42} = 0.01486$	$\mu_\epsilon = 0.4707$	
$\eta = 0.14556$	$\delta_n = 7.4301$	

Table 2: Experimental scattering data involved in CC optical analysis

Reference	Projectile Energy (MeV)	Spin, parity, energy of the excited level $0^+(0.0)$	$2^+(1.454)$	$3^-(4.475)$
Smith et al.[13]	$E_n = 4.5$	•	•	
	5.0	•	•	
	5.5	•	•	
	5.9	•	•	
	6.5	•	•	
	7.14	•	•	
	7.5	○	○	
	8.029	•	•	
	8.399	•	•	
	9.06	○	○	
	9.5	•	•	
Guss et al.[14]	$E_n = 7.904$	○	○	
	9.958	○	○	
	11.952	○	○	
	13.941	○	○	
Tutubalin et al.[15]	$E_n = 14.7$	○		
Perdoni et al.[16]	$E_n = 16.934$	○	○	
Yamanouti et al.[17]	$E_n = 24.0$	○	○	○
Tesmer et al.[23]	$E_p = 20.0$	•	•	
Van Hall et al.[24]	$E_p = 20.4$	•	•	
	24.6	•	•	•
Ridley et al.[18]	$E_p = 30.3$	○		
Stovall et al.[19]	$E_p = 39.7$		○	○
Blumberg et al.[20, 21]	$E_p = 40.0$	○	○	○
Fulmer et al.[22]	$E_p = 61.4$	○		
Sakaguchi et al.[25]	$E_p = 65.0$	•		

○- data used for potential parameter adjustment

•- data used for comparison only

Table 3: The optical potential parameters allowing the best fit of experimental data

$$V_R = 52.33 - 0.394E + 0.00107E^2$$

$$W_D = \begin{cases} 4.40 + 0.126E & E \le 25.75 \\ 7.645 - 0.0577(E - 25.75) & E > 25.75 \end{cases}$$

$$W_V = \begin{cases} 1.16 + 0.057E & E \le 25.75 \\ 2.628 + 0.0547(E - 25.75) & E > 25.75 \end{cases}$$

$V_{so} = 4.80$	$W_{so} = 0.0$	
$r_R = 1.2275$	$a_R = 0.593 + 0.00115E$	
$r_D = 1.1371$	$a_D = \begin{cases} 0.509 + 0.00253E & E \le 25.75 \\ 0.5741 & E > 25.75 \end{cases}$	
$r_V = 1.0967$	$a_V = 0.493 + 0.00426$	
$r_{so} = 1.1232$	$a_{so} = 0.660$	
$r_C = 1.2437$	$a_C = 0.573$	
$C_{Cuol} = 0.493$	$C_{viso} = 0.85$	$C_{wiso} = 3.25$
$\beta_{20} = 0.0788$	$\beta_{30} = \beta_{20}\epsilon_0 = 0.0805$	$\beta_4 = 0.0142$

Strength and incident energy E in MeV; radii and diffusenesses in fm.

References

[1] J. Lee, Y.-O. Lee, E. Sukhovitski, "Program OPTMAN and SHEMMAN Version 6", KAERI/TR-1458/2000 (2000)

[2] E.S. Sukhovitskiĭ, Y.V., S. Chiba., O. Iwamoto, Y.V. Porodzinskiĭ, , Nucl. Phys. **A640**, 147 (1998).

[3] Y.V. Porodzinskiĭ, E.S. Sukhovitskiĭ, Phys. of Atom. Nucl.**59**, 247 (1996).

[4] Y.V. Porodzinskiĭ, E.S. Sukhovitskiĭ, Sov. J. Nucl. Phys. **53**, 41 (1991).

[5] Y.V. Porodzinskiĭ, E.S. Sukhovitskiĭ, Sov. J. Nucl. Phys. **54**, 942 (1991).

[6] F. Iachello and A. Arima, *"The Interating Boson Model"*, Cambridge Univ. Press (1987).

[7] A.S. Davydov and A.A. Chaban, Nucl. Phys. **20**, 499(1960).

[8] S. Chiba., O. Iwamoto, Y. Yamanouti, M. Sugimoto, M. Mizumoto, K. Hasegawa, E.Sh. Sukhovitskiĭ, Y.V. Porodzinskiĭ, Y. Watanabe, Nucl. Phys. **A624**, 305 (1997).

[9] J.M. Eisenberg and W. Greiner, "Nuclear Models", North-Holland, Amsterdam (1970).

[10] E.Sh. Sukhovitskiĭ, Y.V. Porodzinskiĭ, O. Iwamoto, S. Chiba., K. Shibata, Report JAERI-Data/Code 98-019, JAERI (1998).

[11] E.Sh. Sukhovitskiĭ, O. Iwamoto, S. Chiba, K. Shibata, Report JAERI-Data/Code 99-028, JAERI (1999).

[12] H.D. Lemmel, Report IAEA-NDS-1 Rev.7, Vienna (1996).

[13] A.B. Smith, P.T. Guenter, J.F. Whalen, S. Chiba, J. of Phys. **G18**, 624 (1992), for approved data see Report ANL-NDM-120 (1991).

[14] P.P. Guss, R.C. Byrd, C.E. Floyd, C.R. Howell et al., Nucl. Phys. **A438**, 187 (1985).

[15] A.I. Tutubalin, A.P. Kljucharev, V.P. Bozhko, V.Ja. Colovnja et. al., Procced. of 2^{nd} National Soviet Conf. on Neutron Physics, Kiev, May 1973, **v3,** 62, F.E.I., Obninsk, 1974.

[16] R.S. Perdoni, C.R. Howell, C.M. Honore, H.G. Pfutzner et al., Phys.Rev. **C38**, 2052 (1988).

[17] Y. Yamanouti, J. Rapaport, S.M. Grimes, V. Kulkarni et al., Int. Conf. on Nuclear Cross Sections for Technology, Knoxville,Tennessee, Oct 1979, Proceed. publ. as NBS Spec. Publ. **594**, p.146, Sept., 1980.

[18] B.W. Ridley, J.F. Turner, Nucl. Phys. **58**, 497 (1964).

[19] T. Stovall, N.M. Hintz, Phys. Rev. **B135**, 330 (1964).

[20] L.N. Blumberg, E.E. Cross, A. Von Der Woude, A. Zucker, R.H. Bassel, Phys.Rev. **147**, 812 (1966).

[21] M.P. Fricke, E.E. Cross, A. Zucker, Phys. Rev. **181**, 1565 (1969).

[22] C.B. Fulmer, J.B. Ball, A. Scott, M.L. Whitten, Phys. Rev. **163**, 1153 (1967).

[23] J.R. Tesmer, F.H. Schmidt, Phys.Rev. **C5**, 864 (1972).

[24] P.J Van Hall, J.P.M.G. Melssen, S.D. Wassenaar, O.J. Poppema et al., Nucl. Phys. **A261**, 63 (1977).

[25] H. Sakaguchi, M. Nakamura, K. Hatanaka, T. Noro, Phys. Let. **B99**, 92 (1981).

[26] A.Brusegan, G. Rohr, R. Shelley, E. Macavero et al., Proc. Int. Conf. on Nuclear Data for Science and Technology, Gatlinburg, May, 1994, p.224

[27] S. Cierjacks, P. Forti, D Kopsh, L. Kropp et al., Report KFK-1000 (Suppl. 1) (1968) .

[28] F.G. Perey, T.A. Love, W.E. Kinney, Report ORNL-4823, (1972).

[29] D.C. Larson, J.A. Harver, N.W. Hill, Report ORNL-5787 (1981).

[30] F.S. Dietrich, W.P. Abfalterer, R.C. Haight, G.L. Morgan et al., Proc. Int. Conf. on Nuclear Data for Science and Technology, Trieste, 19-24 May, 1997, v. 1, p. 402.

[31] A.J. Koning, J.P. Delaroche and O. Bersillon, ENC-RX-97-047, Netherlands Energy Research Foundation ECN (1997).

[32] S. Raman, C.H. Malarkey, W.T., Milner, C.W. Nestor Jr., P.H. Stelson, Atomic Data and Nucl. Data Tables **36**, 1 (1987).

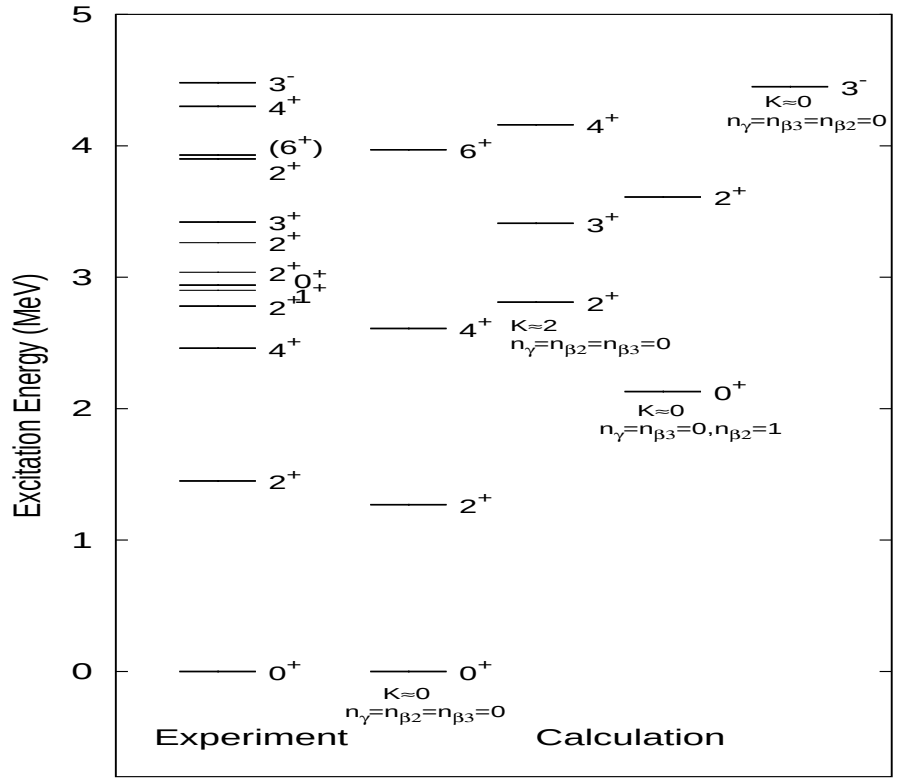

Figure 1: Comparison of the experimental and calculated level schemes. Thick lines show experimental levels describes by the soft-rotator model. Note that above 3.5 MeV excitation energy, due to lack of space and not to overcrowd the figure, we demonstrate only those experimental levels, that are predicted by our model.

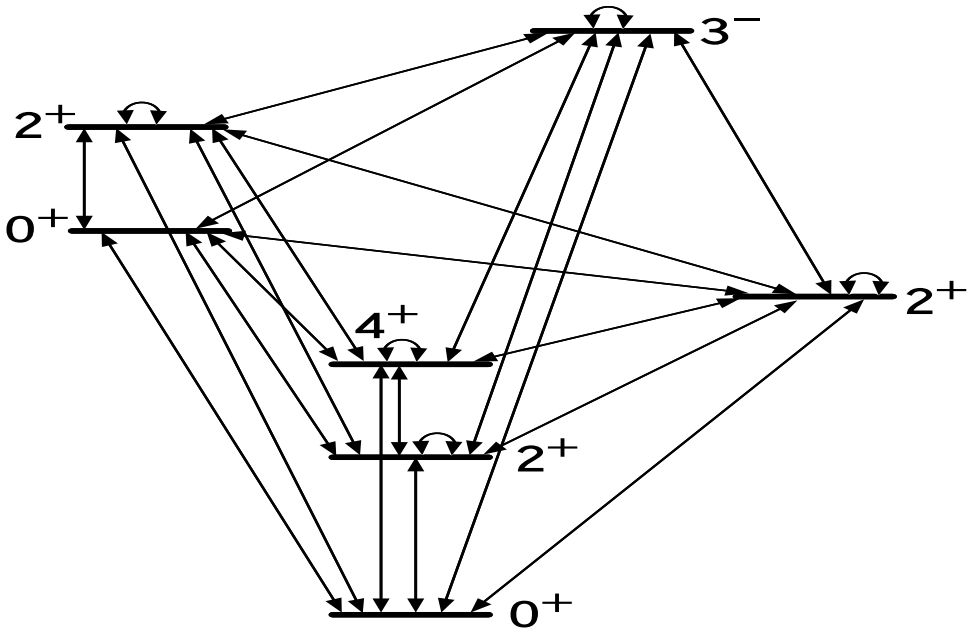

Figure 2: Coupling scheme employed in the present calculation. Arrows show coupling used in the parameter search procedure.

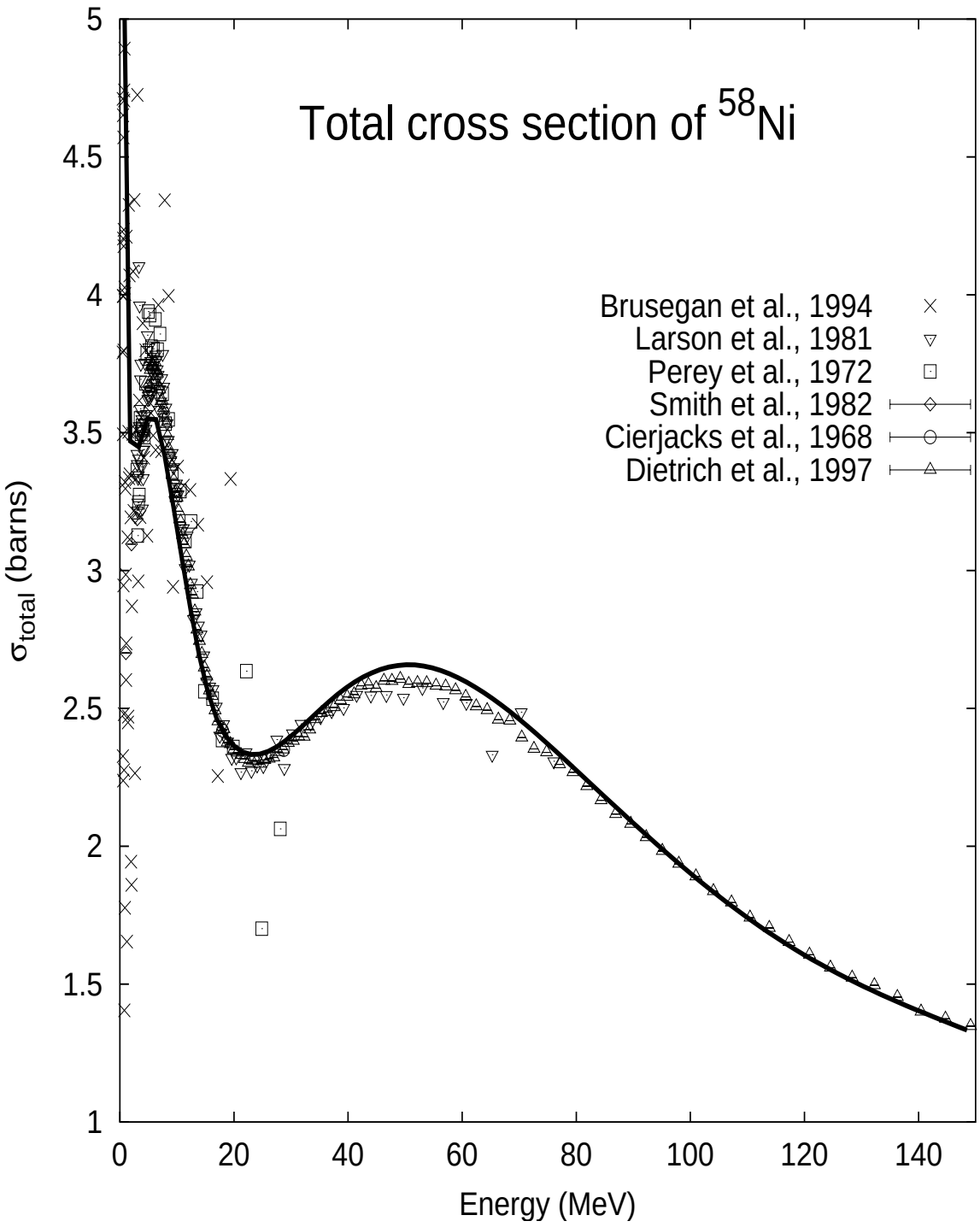

Figure 3: Comparison of experimental and calculated ^{58}Ni total neutron cross sections up to 150 MeV incident energy. Solid line : Present calculation.

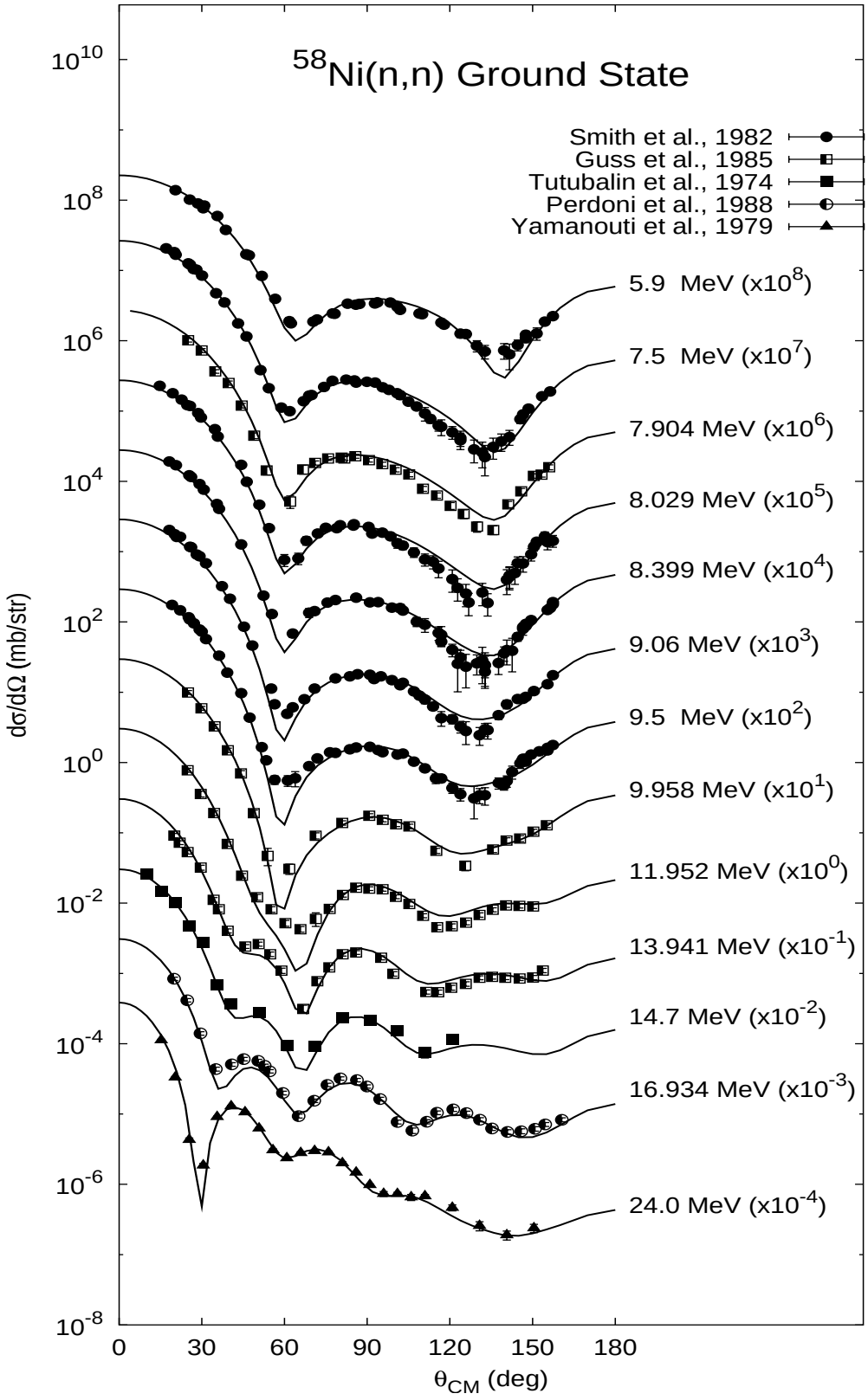

Figure 4: Comparison of experimental and calculated angular distributions for neutrons elastically scattered from ^{58}Ni. Solid lines : Present calculation.

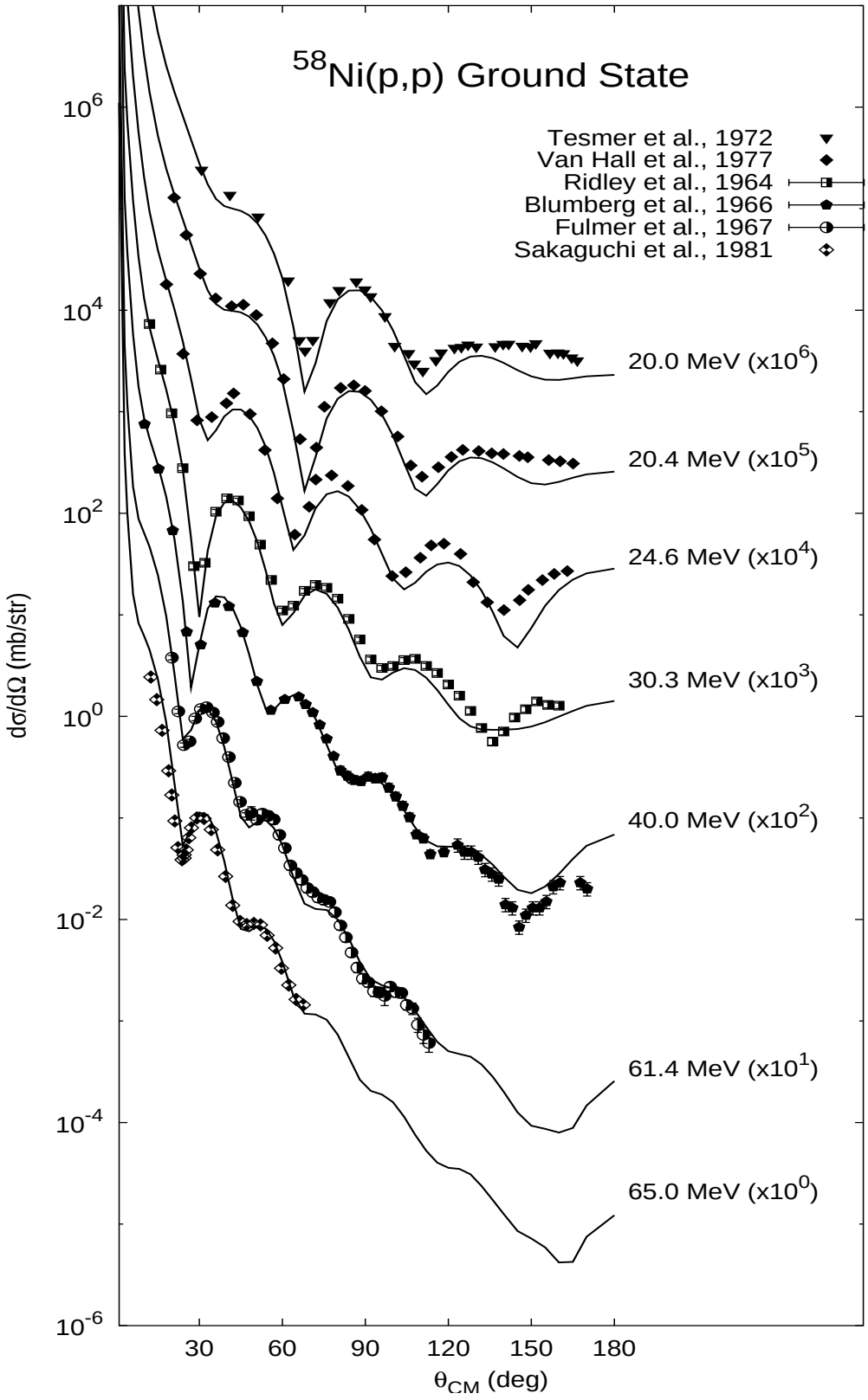

Figure 5: Comparson of experimental and calculated angular distributions for protons elastically scattered from ^{58}Ni. Solid lines : Present calculation.

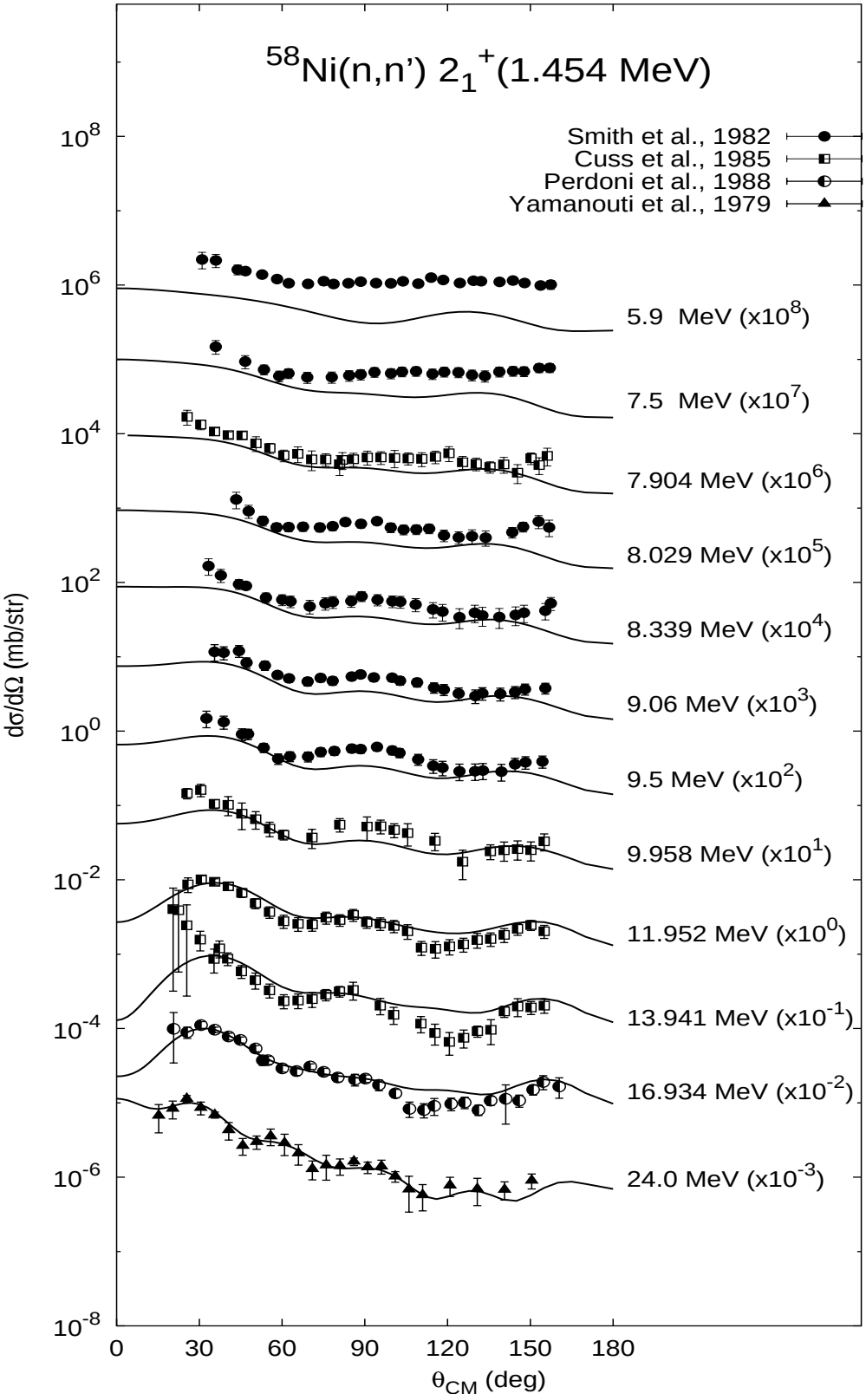

Figure 6: Comparison of experimental and calculated angular distributions for neutrons scattered to the 2^+ (1.454 MeV) level of ^{58}Ni. Solid lines : Present calculation.

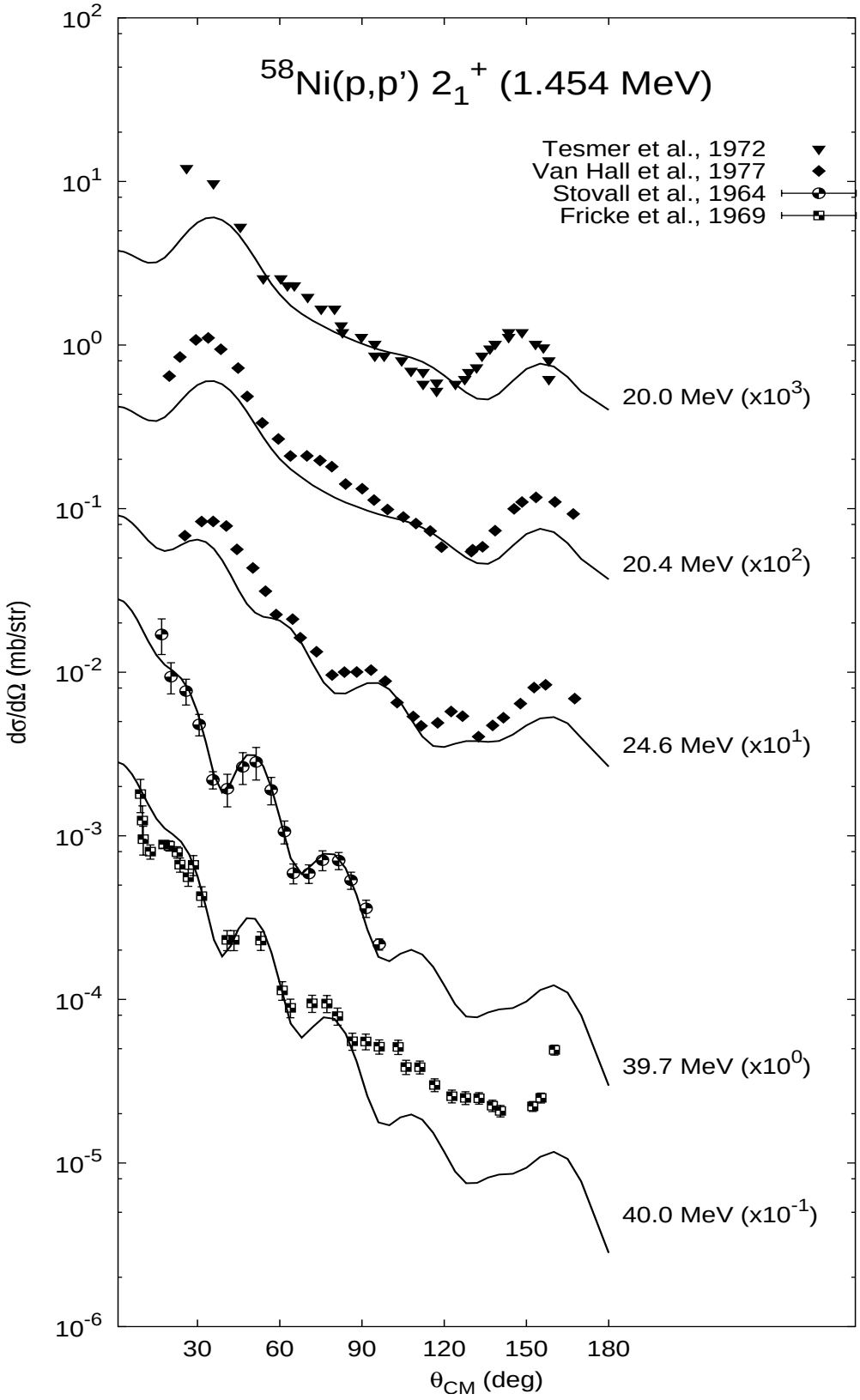

Figure 7: Comparison of experimental and calculated angular distributions for protons scattered to the 2^+ (1.454 MeV) level of ^{58}Ni. Solid lines : Present calculation.

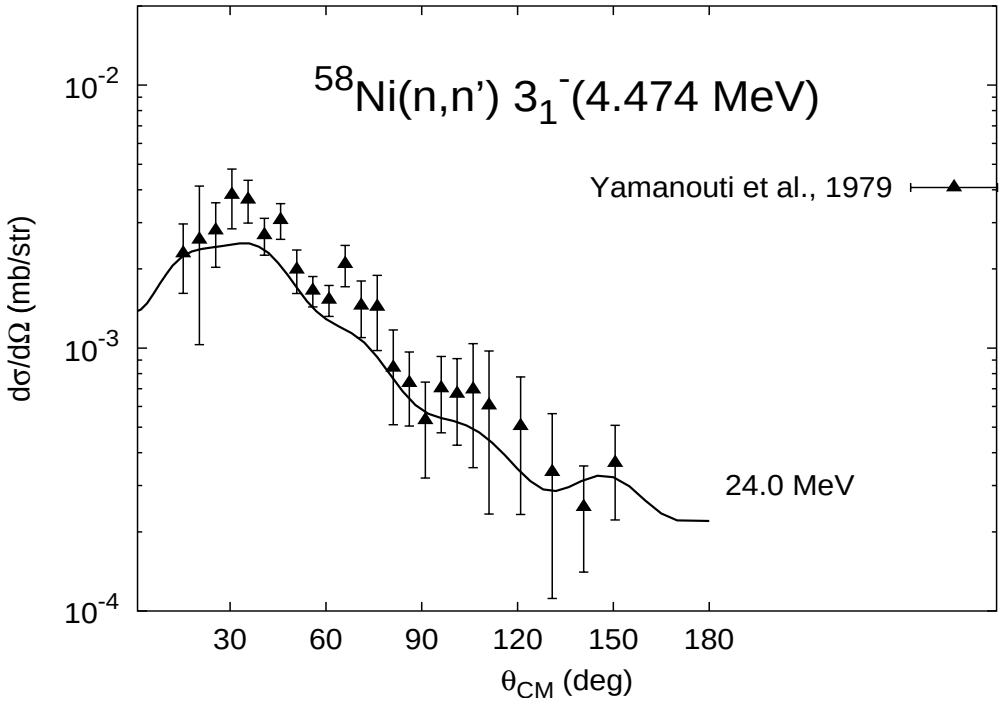

Figure 8: Comparison of experimental and calculated angular distribution for neutrons scattered to the 3^- (4.475 MeV) level of the ^{58}Ni. Solid lines : Present calculation.

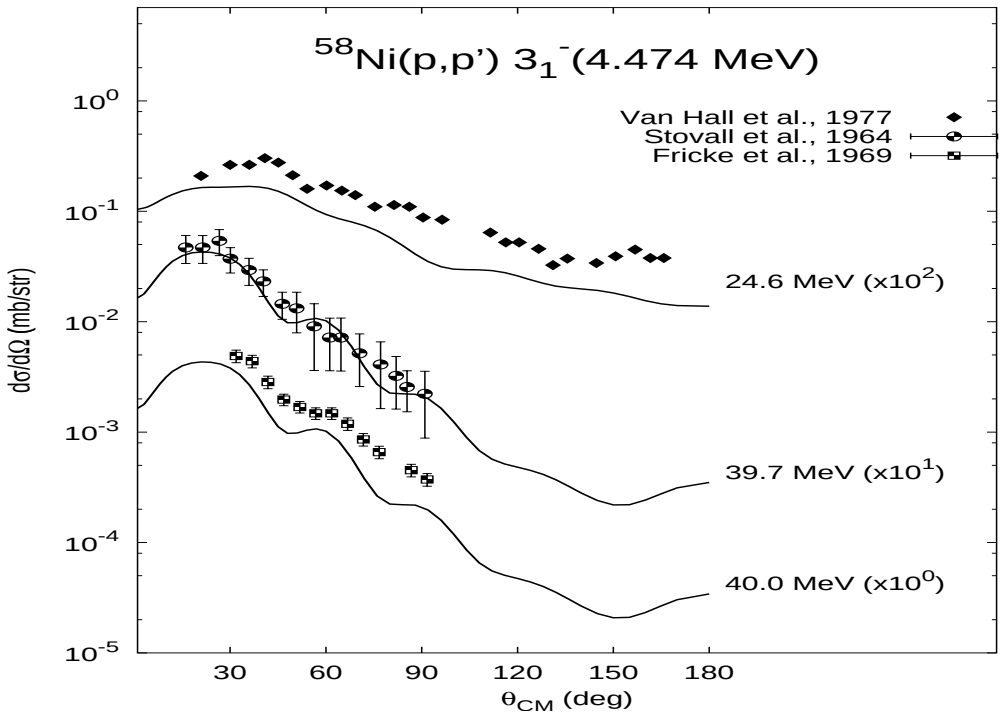

Figure 9: Comparison of experimental and calculated angular distributions for protons scattered to the 3^- (4.475 MeV) level of the ^{58}Ni. Solid lines : Present calculation.